



## A New Design and Implementation of 4x4 Butler Matrix for Ka Band Applications

S.Aourik<sup>(1)</sup>, A.Errkik<sup>(1)</sup>, J.Zbitou<sup>(1)</sup>, M.Latrach<sup>(2)</sup>

(1) MIET Laboratory / Hassan First University of Settat, Morocco

(2) Electronic and Physics Sciences department / RF-EMC research group, ESEO- IETR, Angers, France

### Abstract

This study presents the optimum design of a 4x4 planar Butler matrix array as a central feature of a switched beam smart antenna system operating at 28 GHz for Ka-band applications. The design is developed on a multilayer structure and the antenna arrays are feeding by using slots. In this work the slot optimized and defined on the ground plane to achieve an optimum feeding, with RO3003 substrate of dielectric constant equal to 3 and loss tangent equal to 0.001. In the 4x4 Butler matrix, four input ports are used to feed four networks composed of four microstrip patch antennas creating the beamforming array. Such network can produce four uniform orthogonal beams, at 12°, -12°, 28° and -28°. Design details and simulation results for the components (hybrid coupler, crossover, phase shifter) used to implement the matrix are provided by using two electromagnetic solvers one based on Moements method and the second one on Finite Integration Technique (FIT).

**Index Terms**— Butler matrix, beamforming network, multi-layered, ka-band, microstrip patch antenna array.

### 1 Introduction

Multiple Beam Network antennas feeds play a central role in many antenna applications. In fact, the desire to sweep the beam of an antenna, having a narrow half-power width and a large gain, allows a wide coverage. This desire stems from the increasing complexity of communication and surveillance systems. In response, future communications networks will have to implement increasingly sophisticated techniques. Currently examples such as agile beam radars, satellite or indoor communication systems, ECM jamming systems, illustrate this growing complexity of modern requirements. The use of portions of the spectrum in the millimeter wave region, including frequency bands about 28 and 40 GHz [1- 3], is one of the main aspects of this new generation of communication. Using a higher part of the spectrum will enable high-speed transfer, which leads to new applications where the key factor is low latency and low liability [4-5] , however, the increase in frequency will bring new challenges to the design of communication infrastructure with regard to the reduction of cells. This frequency increase would result greater losses of free space, but also means a reduction in the size of the radiating components making it ideal for the implementation of antenna arrays to compensate the losses of free space [6,

7]. The Butler matrix is one of passive beamforming network consisting of N input/output port and N input/output antenna elements produced N principal orthogonal beam at different locations [8], Due to numerous advantages such as low profile, easy fabrication and low cost, the Butler matrix was easily implemented using the microstrip technique[9-10]. A Butler matrix is a classical beamforming circuit that is commonly used in MIMO systems [11, 12] and it consists of three main elements, a 90° hybrid coupler, a 0 dB crossover and a phase shifter. Several studies have been carried out in recent years on the design and deployment of Butler matrices targeted to the new high frequencies of 5 G technology and in ka-band [13- 14]. In this work we present a design of 4x4 Butler Matrix in multilayer microstrip with slot technical feed for Ka-band, to avoid parasite radiation. The structure contains three layers which are, the feed network made of the Butler matrix and the transmission lines on a substrate RO3003 with thickness of 0.5 mm, a Ground plane containing feed slot and antenna arrays layer on an RO3003 with thickness of 0.2 mm. The paper is organized as following. Section II contains Analysis and design of individual components used in Butler matrix; Section III shows Implementation of Butler matrix with an array of patch antenna. Finally, Section IV where we present the measurement results obtained with the structure.

### 2 Analysis and design of individual components used in Butler matrix

The design and simulation of the Butler matrix operating at the 28 GHz center frequency requires that its various components be studied and characterized. The design and simulation of the Butler matrix operating at the 28 GHz center frequency requires that its various components be studied and characterized, with minimum losses [15]. The efficiency of the matrix directly depends on the performance of its elements.

#### 2.1 Hybrid Coupler Design

The hybrid coupler is the most important component in the Butler matrix [16]. The general structure of coupler is defined in Fig. 1, a and b, the geometry of the directional coupler is studied by the (ADS) Advanced Design System. This structure is a quadrupole allowing the division of an

input signal into two output signals of equal amplitude and  $90^\circ$  phase shift at the frequency of operation. The main line of the coupler is coupled to a secondary line by two-quarter wavelength long sections spaced over one quarter wavelength.

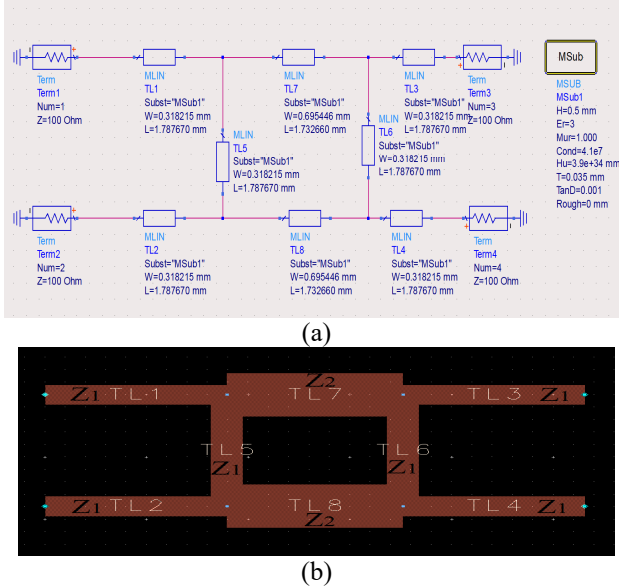


**Figure 1.** Structure of hybrid coupler. (a) schematic Design of the proposed coupler. (b) the layout of the validated coupler.

Typically, the input is at port 1 and the output ports 4 and 3 while the isolated port 2 is terminated in a match load. In this study,  $90^\circ$  hybrid is designed by two ( $Z_1=100\Omega$ ) and two ( $Z_2=70.71\Omega$ ) transmission lines.

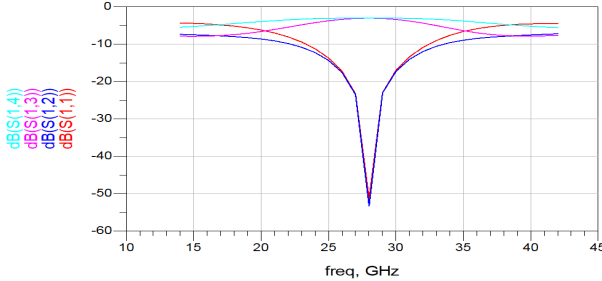


**Figure 2.** S parameters versus frequency for the hybrid coupler.

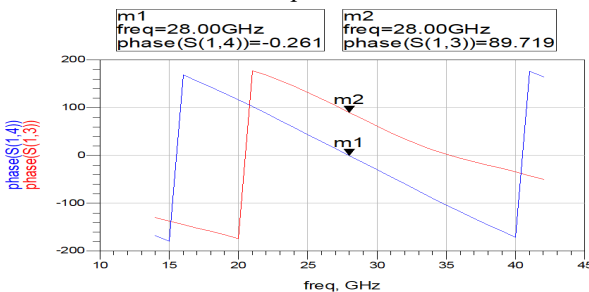


**Figure 3.** The phase difference between port 3 and port 4 for the hybrid coupler.

The simulated magnitudes ( $S_{11}$ ,  $S_{12}$ ,  $S_{13}$ , and  $S_{14}$ ) for the hybrid coupler are  $-50\text{dB}$ ,  $-53\text{dB}$ ,  $-3\text{dB}$  and  $-3\text{dB}$

respectively as shown in Fig. 2. As expected, the phase difference between port 3 and port 4 is  $89.7^\circ$  (Fig. 3). The coupler's electromagnetic simulation results are important. In addition, the coupler has good impedance matching.

## 2.2 Crossover

In the realization of the Butler matrix, crossover is the biggest challenge [17]. We must use a crossover with a good level of isolation between the input ports to avoid overlapping signals at crossings. It can be built simply by cascading two hybrid couplers [18], in this work we chose to put a quarter wave line between them in order to have a good isolation. In the same way, the crossover has been designed in schematic using  $100\Omega$  microstrip transmission lines as shown in Fig. 4, shown the layout geometry of crossover.

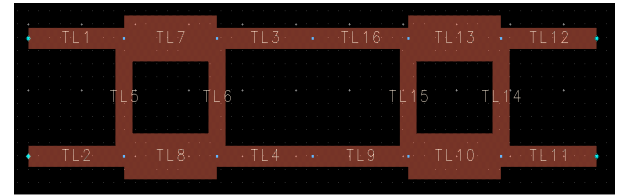


**Figure 4.** Structure of proposed crossover.

The insertion loss for the coupled port S13 is  $-0.1\text{ dB}$  while return loss S11 is  $-58\text{ dB}$  and the isolated ports S12 and S14 are  $-46\text{ dB}$  and  $-66\text{ dB}$  respectively for the frequency of interest (Fig. 5). These results are satisfactory in terms of reflection and isolation parameters.

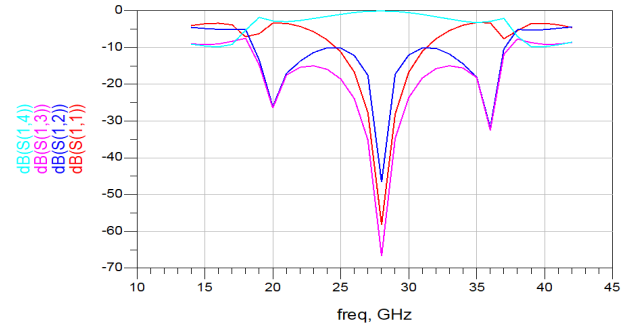


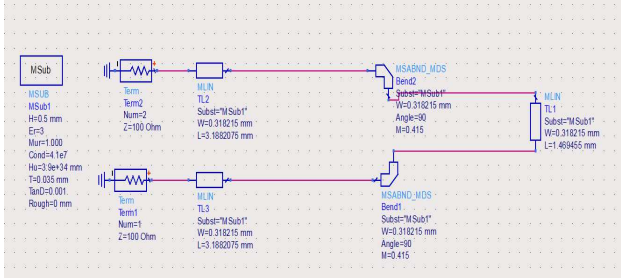
**Figure 5.** S parameters versus frequency for the crossover.

## 2.3 Phase shifter

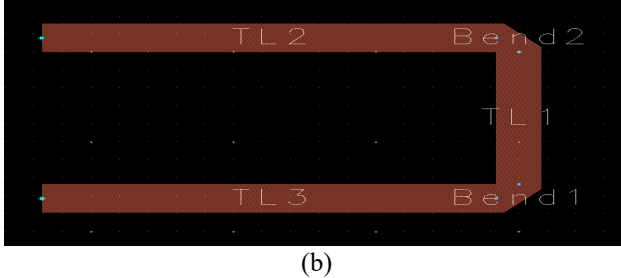
The microstrip line has a certain wavelength guided at a frequency. To create a phase  $\theta$  delay with one microstrip line compared to another, we therefore add an additional line length  $\Delta L$ .

$$\Delta L = \frac{\theta * \lambda_g}{360} \quad (1)$$

Where the  $\lambda_g$  denotes the guided wavelength. The optimum design for  $100\Omega$  microstrip line with  $45^\circ$  phase shift was achieved schematic and layout as shown in Fig. 6.



(a)



(b)

**Figure 6.** Structure of phase shifter. (a) schematic. (b) layout.

As shown in Fig. 7, Insertions loss represented by S11 parameter is -0.08 dB, while the return loss S11 is -26 dB at 28 GHz.

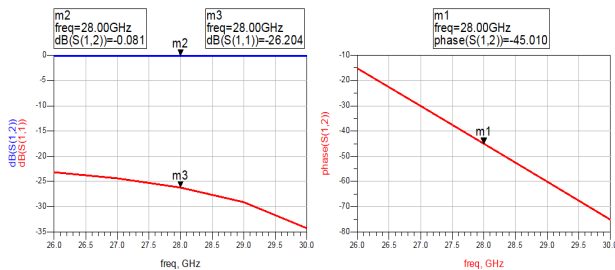


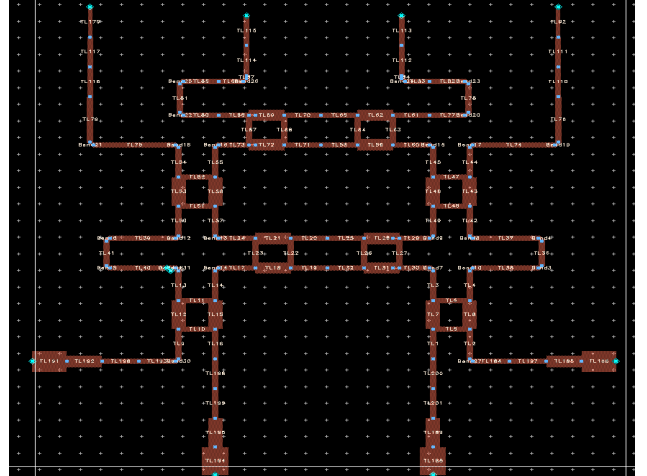
**Figure 7.** S parameters and Simulated phase difference between the ports1 and 2.

For the phase shift, the simulation result is shown in Fig. 7. The phase difference between the ports1 and 2 is 45° at the desired frequency.

### 3 Implementation of Butler matrix with an array of patch antenna.

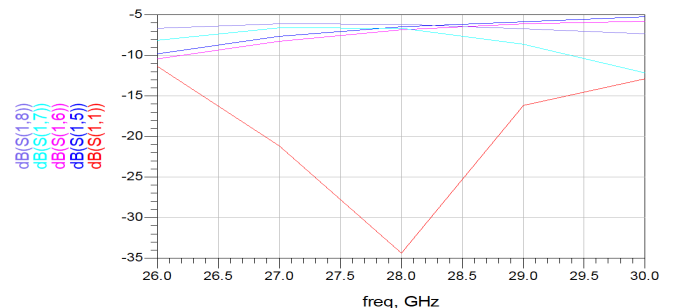
#### 3.1 Butler matrix

Fig. 8. presents the layout of the proposed 4\*4 Butler matrix. The proposed Butler matrix, combining the components that we presented before after, Hybrid coupler, Crossover, Phase shifter. was designed as a passive microstrip array on the same substrate RO3003.



**Figure 8.** The layout of the proposed Butler matrix.

The proposed Butler matrix was treated as a beam forming network, as various input ports were excited, which provided four output signals with equal power levels and progressive stages, as shown in Fig. 9, at the center frequency of 28 GHz. Hence, by stimulating the designated input port, the user can switch the direction of the main radiation beam. The system can produce multiple narrow beams in different directions and there by selecting the strongest signal among all the available signals. Fig. 10, shows simulation results of port 1 insertion loss and return loss when matching the other ports. These results illustrate that the return loss is better than -33 dB and the coupling to the output ports is 7 dB. It can be concluded that the results obtained are highly promising.



**Figure 9.** Simulated results of S parameters of the 4 × 4 Butler matrix when port 1 is fed.

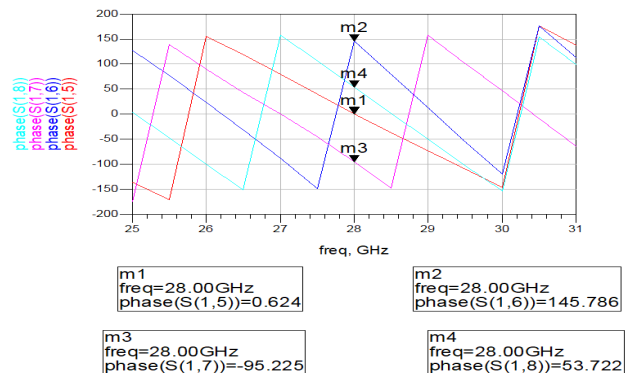


**Figure 10.** Simulated phase differences between port 1 and 5, 1 and 6, 1 and 7, 1 and 8.

### 3.2 Array antennas

The technique of feeding directly in contact on the same side of the radiating elements by microstrip lines in the millimeter range is not effective [19] because the parasite radiation created by the matrix component. A second technique consists of developing arrays of plated antennas fed through slots of microstrip lines, each radiating element being associated with its own feed line [20]. This method helps prevent stray line radiation which can, in some cases, disrupt side-lobe levels and increase cross-component levels. The geometric description of the antenna is specified in the Fig. 11.

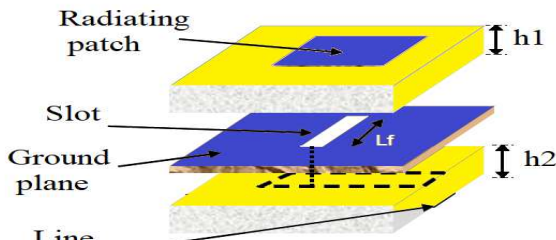


**Figure 11.** Exploded view of slot fed antenna.

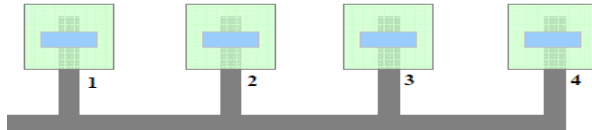


**Figure 12.** Architecture of the feed network.

The antenna is made of two identical RO3003 substrates with different thicknesses  $h_1 = 0.2$  mm and  $h_2 = 0.5$  mm. The low substrate heights are selected to prevent the strong excitations of the surface waves. we have chosen a serial antenna network its architecture presented in Fig. 12, the patch excitation is done by slot and the network feed will be in series. In order to guarantee a very good feeding for the radiating elements and to minimize the losses caused by the lines and the substrate, a study was made on the geometry of the slot and its dimension. The Fig. 13, shows new slot geometry has been studied, based on a circle which allow us to have a very good current circulation between the two substrates.

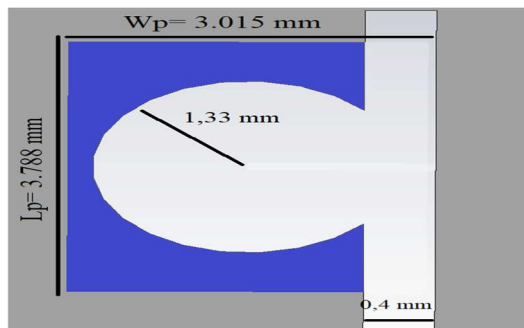


**Figure 13.** Architecture of feeding slot on ground plane.

Distribution of the current density at the ground plane level showed in the fig.14, we can mark a good current flow in the slots which ensures a good supply of the antennas.

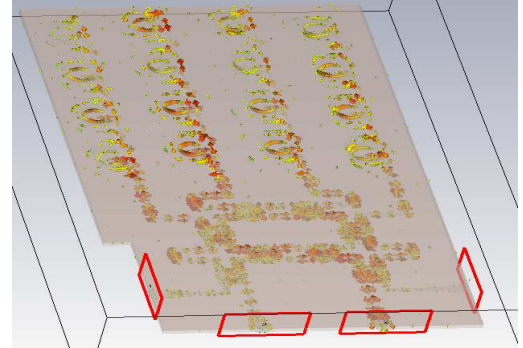


**Figure 14.** Current distribution on ground plane at 28 Ghz.

Fig. 14, shows the 3D of the proposed multilayer  $4 \times 4$  patch array with the  $4 \times 4$  Butler matrix, in which four  $1 \times 4$  patch sub-arrays are excited by the slot-coupled center-fed structure. Two substrates RO3003 were used in the structure with different thicknesses  $h_1$  and  $h_2$ .

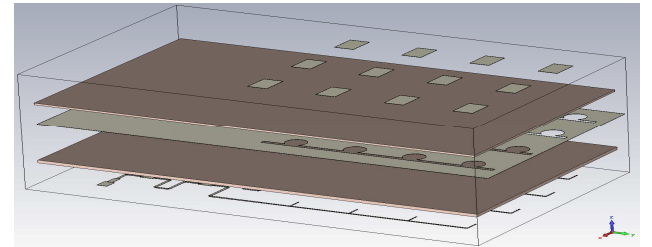


**Figure 15.** Configuration of proposed structure in 3D.

## 4 Experimental results

A modification was necessary, where the more external input and output lines (Ports 1, 4, 5 and 8) are extended in order to make space to allocate the connectors, while keeping the same phase properties. Fig. 15, show the measured and simulated S parameters of input ports. The effect of the substrates has been included in the simulated results. As indicated, the measured return losses are less than -10 dB within the operating frequency range 28 GHz.

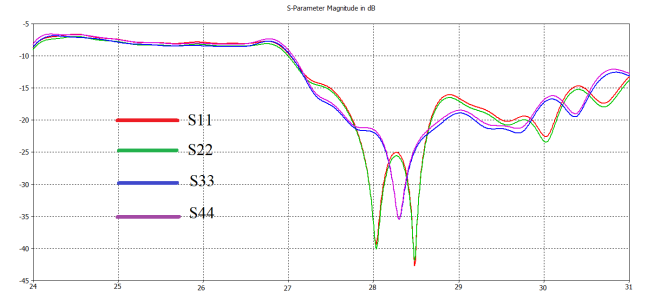


**Figure 16.** Return Loss  $S_{11}$ ,  $S_{22}$ ,  $S_{33}$ ,  $S_{44}$  at Port 1, 2, 3 and 4 respectively.

Fig. 16, shows the simulated H-plane radiation patterns of the multi-beam antenna array at 28 GHz. When Port 2 and Port 3 were individually excited, the simulated main beam

pointed to the directions of  $12^\circ$  and  $-12^\circ$ , respectively, with the gains of 9.8 dBi and 7.8 dBi. The excitations of P1 and P4 in turn resulted in the measured main beam pointing to the directions of  $29^\circ$  and  $-29^\circ$ , respectively, with the gains of 10.1 dBi and 9.9 dBi.

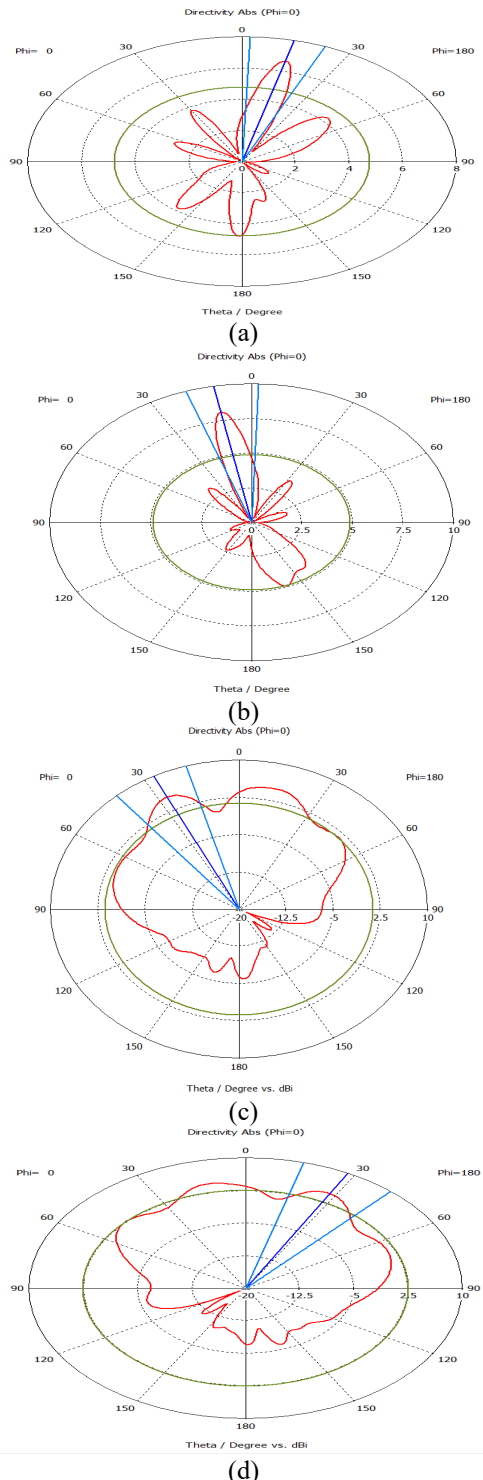


**Figure 17.** Simulated H-plane patterns excited by different input ports at 28 GHz: (a) P2 ( $12^\circ$ ), (b) P3 ( $-12^\circ$ ), (c) P1 ( $29^\circ$ ), and (d) P4 ( $-29^\circ$ ).

## 5 Conclusion

The 4x4 Butler matrix and its components were studied and simulated in order to be integrated in a general multilayer structure to feed the four antenna arrays, each of these latter contains four identical radiating elements at 28 GHz. The structure was achieved by using the multilayer structure technique permitting a separation between the feeding and the radiation parts. In this work a new slot has been used on a circle shape to obtain a good radiating element feeding. Simulated results of radiation patterns show that the  $4 \times 4$  Butler Matrix can provide an adequate phase difference and an acceptable amplitude to the antenna array in order to function as a beamforming network in the frequency range of interest. Such achieved circuit is suitable for applications in the Ka band.

## 6 References

1. Technical Report 16-89, Federal Communications Commission, 07 2016.
2. T. S. Rappaport, S. Sun, R. Mayzus, H. Zhao, Y. Azar, K. Wang, G. N. Wong, J. K. Schulz, M. Samimi, and F. Gutierrez. Millimeter wave mobile communications for 5G cellular: It will work! *IEEE Access*, 1:335–349, 2013. ISSN 2169-3536. doi: 10.1109/ACCESS.2013.2260813.
3. 3GPP. Release description; Release 15. Technical specification (ts), 3rd Generation Partnership Project (3GPP), 03 2019. TR 21.915.
4. I. Parvez, A. Rahmati, I. Guvenc, A. I. Sarwat, and H. Dai. A survey on low latency towards 5g: Ran, core network and caching solutions. *IEEE Communications Surveys Tutorials*, 20(4), Fourthquarter 2018. ISSN 2373-745X. doi: 10.1109/COMST.2018.2841349.
5. D. Soldani, Y. J. Guo, B. Barani, P. Mogensen, C. I, and S. K. Das. 5g for ultra-reliable low-latency communications. *IEEE Network*, 32(2): 6–7, March 2018. ISSN 1558-156X. doi: 10.1109/MNET.2018.8329617.
6. A. L. Swindlehurst, E. Ayanoglu, P. Heydari, and F. Capolino. Millimeter-wave massive mimo: the next wireless revolution? *IEEE Communications Magazine*, 52(9):56–62, Sep. 2014. ISSN 0163-6804.
7. R. Daniels J. Murdock T. Rappaport, R. Heath Jr. Millimeter wave wireless communications. Pearson Education, 1 edition, 9 2014. ISBN 978-0132172288.
8. Ng Chee Tiong Desmond, “Smart Antennas for Wireless Applications and Switched Beamforming,” Department of Information Technology and Electrical Engineering the University of Queensland, 2001.
9. R. Garg, Microstrip Antenna Design Handbook, Artech House Books, Nov 2000.
10. Li "Switched-beam antenna based on modified butler matrix with Low sidelobe level" *Electronics Letters*, vol. 40 No. 5, 4th March 2004.
11. A. Grau, J. Romeu, S. Blanch, L. Jofre, and F. De Flaviis. Optimization of linear multielement antennas for selection combining by means of a butler matrix in different MIMO environments. *IEEE Transactions on Antennas and Propagation*, 54(11):3251–3264, Nov 2006. ISSN 0018-926X. doi: 10.1109/TAP.2006.883971.

12. P. Chen, W. Hong, Z. Kuai, J. Xu, H. Wang, J. Chen, H. Tang, J. Zhou, and K. Wu. A multibeam antenna based on substrate integrated waveguide technology for MIMO wireless communications. *IEEE Transactions on Antennas and Propagation*, 57(6):1813–1821, June 2009. ISSN 0018-926X. doi: 10.1109/TAP.2009.2019868.
13. Nishesh Tiwari and Thipparaju Rama Rao. A switched beam antenna array with butler matrix network using substrate integrated waveguide technology for 60 GHz wireless communications. *AEU - International Journal of Electronics and Communications*, 70(6):850 – 856, 2016. ISSN 1434-8411. doi: <https://doi.org/10.1016/j.aeue.2016.03.014>.
14. J. Zhu, B. Peng, and S. Li. Cavity-backed high-gain switch beam antenna array for 60-ghz applications. *IET Microwaves, Antennas Propagation*, 11(12):1776–1781, 2017. ISSN 1751-8733.
15. Tayeb A. Denidni and Taro Eric Liber "Wide Band Four-Port Butler Matrix for SwitchedMultibeam Antenna Arrays" *IEEE*, vol. 14, pp.2461-2464, 2003.
16. G Srivastava and V. Gupta, "Microwave devices and circuit design," New Delhi: Prentice-Hall of India, 2006.
17. A. Tajik, A. Shafiei Alavijeh and M. Fakharzadeh, "Asymmetrical 4\*4 Butler Matrix and its Application for Single Layer 8\*8Butler Matrix," in *IEEE Transactions on Antennas and Propagation*, vol. 67, no. 8, pp. 5372-5379, Aug. 2019, doi: 10.1109/TAP.2019.2916695.
18. Pozar, D.M, Microwave Engineering. 3rd Edn, John wily and sons, New York, 2005.
19. D.M. POZAR, "Analysis of an infinite phased array of aperture coupled microstrip patches", *IEEE Transaction an Antennas and Propagation*, vol. 37, pp. 418-425,April 1989.
10. S. Trinh-Van, J. M. Lee, Y. Yang, K. Lee, and K. C. Hwang. A sidelobe-reduced, four-beam array antenna fed by a modified  $4 \times 4$  butler matrix for 5G applications. *IEEE Transactions on Antennas and Propagation*, 67(7):4528–4536, 2019.